ChemPubSoc Europe

DOI: 10.1002/chem.201402890

CHEMISTRY
A European Journal
Full Paper

Protein Aggregates

Pentameric Thiophene-Based Ligands that Spectrally Discriminate Amyloid-β and Tau Aggregates Display Distinct Solvatochromism and Viscosity-Induced Spectral Shifts

Rozalyn A. Simon,[a] Hamid Shirani,[a] K. O. Andreas Åslund,[a] Marcus Bäck,[a] Vahram Haroutunian,[b] Sam Gandy,[b] and K. Peter R. Nilsson*[a]

Abstract: A wide range of neurodegenerative diseases are characterized by the deposition of multiple protein aggregates. Ligands for molecular characterization and discrimination of these pathological hallmarks are thus important for understanding their potential role in pathogenesis as well as for clinical diagnosis of the disease. In this regard, luminescent conjugated oligothiophenes (LCOs) have proven useful for spectral discrimination of amyloid-beta (Aβ) and tau neurofibrillary tangles (NFTs), two of the pathological hallmarks associated with Alzheimer's disease. Herein, the solvatochromism of a library of anionic pentameric thiophene-based ligands, as well as their ability to spectrally discriminate Aβ and tau aggregates, were investigated. Overall, the results from this study identified distinct solvatochromic and viscosity-dependent behavior of thiophene-based ligands that can be applied as indices to direct the chemical design of improved LCOs for spectral separation of Aβ and tau aggregates in brain tissue sections. The results also suggest that the observed spectral transitions of the ligands are due to their ability to conform by induced fit to specific microenvironments within the binding interface of each particular protein aggregate. We foresee that these findings might aid in the chemical design of thiophene-based ligands that are increasingly selective for distinct disease-associated protein aggregates.

Introduction

Conjugated polymers have many unique photophysical properties which render them useful in a variety of applications within the fields of chemistry, molecular biology, and medicine. Luminescent conjugated polymers (LCPs) account for a growing number of developing sensors and probes as their unique properties make them useful reporters in the detection of ions, DNA, and proteins, to name just a few.[1–4] These sensors mainly employ the efficient light harvesting properties or the conformation-sensitive optical properties of the LCPs. The latter is particularly observed for LCPs with a repetitive flexible thiophene backbone, as conformational restriction of the thiophene rings leads to a distinct optical fingerprint.[5]

In recent studies, it has been shown that LCPs can function as target-specific chameleons that change color depending on the structural motif of the target molecule, even in complex samples, such as tissue sections.[6–8] This intrinsic property of LCPs make them useful as selective probes for identifying and distinguishing protein deposits consisting mainly of fibrils with a repetitive cross-β sheet structure. Accumulation of such proteinaceous deposits is the histopathological hallmark of several devastating diseases, including Alzheimer's disease (AD) and prion diseases.[9,10] In addition, novel chemically defined thiophene scaffolds, denoted luminescent conjugated oligothiophenes (LCOs), have been utilized as specific ligands for a variety of disease-associated protein aggregates, as well as for optical in vivo imaging of protein aggregates in real time.[11–16]

Anionic LCOs have proven particularly useful for spectral discrimination of amyloid beta (Aβ) deposits and tau neurofibrillary tangles (NFTs), the two major pathological hallmarks of AD.[11,12,17] Ligands with molecular scaffolds other than thiophene showing selectivity towards tau or Aβ deposits have also been presented and these studies showed that minor chemical alterations of the molecular scaffold could influence the specificity toward either tau or Aβ aggregates.[18,19] Recently, aminonaphthalenyl 2-cyanoacrylate-based probes were also shown to fluorescently discriminate between different types of protein deposits in brain tissue.[20] The discriminating capability

[a] R. A. Simon, Dr. H. Shirani, Dr. K. O. A. Åslund, Dr. M. Bäck, Dr. K. P. R. Nilsson
Department of Chemistry, Linköping University
581 83 Linköping (Sweden)
E-mail: petni@ifm.liu.se

[b] Prof. V. Haroutunian, Prof. S. Gandy
Department of Psychiatry and Alzheimer's Disease Research Center
Mount Sinai School of Medicine, New York, NY 10029 (USA) and
James J. Peters VA Medical Center, Bronx, NY 10468 (USA)

Supporting information for this article is available on the WWW under http://dx.doi.org/10.1002/chem.201402890.

of these dyes was due to the stabilization of the ground versus excited states of these probes as a function of the polarity of the binding pocket on the amyloid. Hence, although most protein deposits share a repetitive cross-β sheet structure, possible differences in the binding pocket microenvironments should be considered when designing ligands towards distinct protein aggregates.

In previous comparisons of structurally related LCOs, it was suggested that for optimal spectral separation of Aβ deposits and tau tangles, an LCO-based ligand should comprise a conformationally flexible backbone consisting of five to seven thiophene units and terminal carboxyl groups extending the conjugated thiophene backbone.[12,17] Upon binding to protein aggregates, LCOs also exhibit decreased Stokes shifts, red-shifted excitation maxima and blue-shifted emission maxima compared to free dyes in solution.[11,12,17] In an effort to elucidate the specific structural features that contribute to enhanced spectral separation between protein aggregates and the photophysical behavior of LCOs bound to protein deposits in more detail, we herein investigated solvatochromism and the effects of solvent viscosity on a group of structurally similar, pentameric, anionic oligothiophene probes. LCOs that displayed spectral variations for Aβ deposits and NFTs also showed distinct solvatochromism and decreased Stokes shifts due to increased solvent viscosity. Hence, these photophysical assessments might aid in the design of LCOs for sensitive optical discrimination of Aβ and tau deposits.

Results and Discussion

Solvatochromism of a library of anionic LCOs

Solvatochromic behavior of small amyloid ligands can be used to approximate the amyloid fibril binding site polarity, as well as the relative change in the dipole moment for individual ligands.[20–23] Therefore, we tested the solvatochromic behavior of a subset of previously reported anionic pentameric LCOs (Figure 1).[11,12,17]

These LCOs were chosen as their molecular composition varies in anionic substitution patterns and in backbone rigidity, as well as in terminal functional groups extending the thiophene backbone. To assess the solvent sensitivity of these LCOs, Lippert–Mataga plots (Stokes shift vs. orientation polarizability) were used.[24] The relative slopes of the fitted lines allows for a comparison of the solvent sensitivity of each of the LCOs tested by means of the orientation polarizability, Δf, for each solvent, determined by the equation:

$$\Delta f = \frac{\varepsilon - 1}{2\varepsilon + 1} - \frac{n^2 - 1}{2n^{+1}}$$

in which ε is the dielectric constant and n the refractive index of each solvent. The calculated Δf values are shown in Table S1

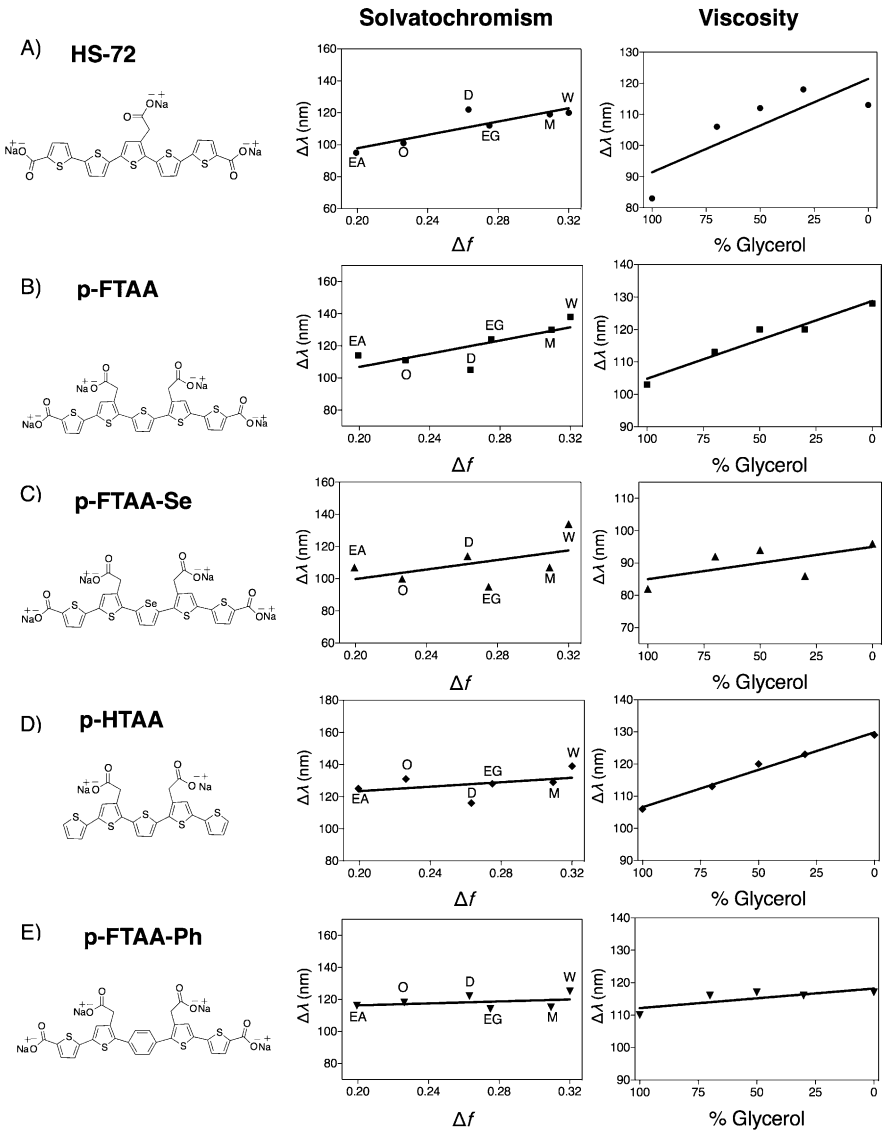

Figure 1. Chemical structures, Lippert–Mataga solvatochromism plots and viscosity plots of the pentameric LCOs: A) HS-72, B) p-FTAA, C) p-FTAA-Se, D) p-HTAA and E) p-FTAA-Ph. For the solvatochromism, solvents of increasing polarity in the following order: ethyl acetate, octanol, dimethyl sulfoxide (DMSO), ethylene glycol, methanol, and water were used. For the viscosity experiments, LCOs were mixed in solutions of ethylene glycol and glycerol with increasing concentrations of glycerol. The LCO concentration was 300 nM for all experiments.

(in the Supporting information). The Stokes shifts, $\Delta\lambda$, were given by:

$$\Delta\lambda = \lambda_{EX} - \lambda_{EM}$$

where λ_{EX} and λ_{EM} are the wavelengths corresponding to the excitation or the emission maximum, respectively.

The results from the solvatochromism study are shown in Figure 1 and Table 1. p-FTAA and HS-72 displayed the highest slope values as these dyes have the highest degree of conformational freedom along the backbone and carboxyl groups extending the thiophene backbone. When the central thiophene ring was replaced with a selenophene (p-FTAA-Se), the relative slope was decreased and still further reduced through the introduction of a central phenyl (p-FTAA-Ph). Reduction in the relative slopes of the fitted lines was also observed when replacing the terminal carboxyl groups with hydrogen (p-HTAA). The combination of chromophore planarization and polarization occurs in natural processes, such as the chemistry of vision,[25,26] and earlier studies[27,28] have also shown that similar phenomena occur in tetrameric oligothiophenes. Thus, conformational restrictions of the LCO backbone will most likely influence the polarization of the dye, since chromophore planarization and polarization are coupled processes. Likewise, substituting the polarizable carboxyl groups with hydrogen atoms will influence the polarization of the molecule and the solvent sensitivity. Furthermore, the carboxyl groups can also acts as π-acceptors. A previous study,[17] comparing p-FTAA, HS-72, p-FTAA-Se and p-FTAA-Ph, has shown that p-FTAA and HS-72 are efficient for spectral discrimination of Aβ deposits and NFTs, whereas p-FTAA-Se was less effective, and p-FTAA-Ph completely lacked the ability to distinguish the two aggregated species. In addition, carboxyl groups extending the conjugated thiophene backbone have been shown to be an additional molecular determinant for achieving optimal spectral separation of Aβ deposits and NFTs.[12] Overall, the trend in solvatochromic behavior of the LCOs supports a correlation between the solvent sensitivity of the LCOs and their ability for spectral separation of Aβ deposits and tau tangles.

As solvatochromism Stokes shifts can provide insights regarding protein binding site polarity,[19,21] we next compared the Stokes shifts obtained from the solvatochromism experiments with the Stokes shifts from the LCOs bound to recombinant Aβ1–42 fibrils (Table 1). All the LCOs, except for p-FTAA-Ph, displayed considerably reduced Stokes shifts for Aβ1–42 fibrils compared to ethyl acetate, indicating that the Aβ1–42 binding pocket is substantially more nonpolar than ethyl acetate ($\varepsilon = 6.08$). In a recent study,[20] using aminonaphthalene 2-cyanoacrylate dyes, the dielectric constants of the binding pocket of Aβ deposits in tissue was determined to be roughly similar to diethyl ether ($\varepsilon = 4.27$) and in a similar study[23] using Nile Red, the Aβ1–42 fibrils binding site polarity was predicted to have a dielectric constant lower than eight.

Previous studies indicate that molecules exhibiting abnormally low Stokes shift are most likely undergoing secondary effects, such as hydrogen bonding or binding-induced conformational restrictions.[24] Thus, the low Stokes shifts observed for the LCOs bound to recombinant Aβ1–42 fibrils might also be due to such secondary effects. In fact, p-FTAA-Ph displayed a similar Stokes shift for Aβ1–42 fibrils as the solvents, and this dye has less conformational freedom than the other LCOs so it is most likely prevented from undergoing additional conformational restriction upon binding to the fibrils. Furthermore, in contrast to the solvent shifts, Aβ1–42 binding also caused a significant bathochromic shift in the excitation spectra for all the LCOs except p-FTAA-Ph, indicating that a planarization of the ground state of the probes occurs upon interaction with the fibrils (Supporting Information Figure S1).

Table 1. Slope values of solvatochromism and viscosity plots (Figure 1, columns 2 and 3).[a]

LCO	Slope: solvent	Slope: viscosity	Stokes shift ethyl acetate	Stokes shift glycerol	Stokes shift Aβ1–42 fibrils
HS-72	208.7	30.0	95	83	51
p-FTAA	205.7	23.0	114	103	48
p-FTAA-Se	148.3	10.0	107	82	54
p-HTAA	69.0	23.3	125	106	46
p-FTAA-Ph	30.7	6.03	116	110	116

[a] Stokes shifts of the most nonpolar solvent (ethyl acetate) and the most viscous solvent (glycerol) are given for comparison to Aβ1–42 fibrils.

Viscosity-dependent excitation and emission profiles of anionic LCOs

As the considerably reduced Stokes shifts observed for LCOs bound to Aβ1–42 fibrils could be due to conformational restrictions within the binding pocket, we proceeded to investigate the role of such restrictions on Stokes shift upon fibril binding using a solvent-viscosity model. Solvent viscosity can be used to assess probe behavior based on conformational restrictions,[24,29] since highly viscous solvents exhibit slow solvent reorientation, restrict conformational freedom, and reduce vibrational modes of relaxation, resulting in emission before complete solvent reorientation and a hypsochromic shift of the probe's emission spectra. In some cases, increasing viscosity can also stabilize the ground state, causing a bathochromic shift in the excitation spectra and further reducing the Stokes shift. By using two solvents of similar polarity (ethylene glycol and glycerol), but with differing viscosities, we were able to simulate the conformational restrictions with minimal changes in polarity. For p-FTAA and HS-72, increasing the ratio of glycerol to ethylene glycol resulted in a red-shift of the excitation spectrum and blue-shift of the emission spectrum (Figure 2). Hence, both of these dyes displayed a viscosity-dependent decrease in their Stokes shifts and considerable Stokes-viscosity slopes, when plotting the Stokes shifts versus percent of glycerol (Figure 1, Table 1). p-HTAA also displayed a substantial Stokes-viscosity slope, although the blue-shift in the emission spectrum was less pronounced. In contrast, p-FTAA-Se and p-FTAA-Ph, displayed minor Stokes-viscosity slopes. As mentioned above, p-FTAA-Ph with a central phenyl

ring has restricted degrees of conformational freedom and for p-FTAA-Se, replacement of the sulfur atom with selenium in the central ring causes the central portion of the backbone to be more planar and less flexible. Compared to the solvatochromism experiments, the viscosity measurements better reflect Stokes shift changes upon conformational restriction of the molecule. Here it becomes more apparent that p-FTAA-Ph and p-FTAA-Se, displayed reduced chromic responsiveness due to inherent conformational restrictions of the conjugated backbone.

Although the effort of increasing the conformational restrictions with viscosity reduced the Stokes shift, the spectral changes that occur upon binding to Aβ1–42 fibrils cannot be reproduced by solvent-only restrictions (Figure 2, Table 1). The occurrence of vibronic peaks, the bathochromic excitation shift, and the hypsochromic emission shift all indicate that the LCOs are much more constrained in the ground state upon binding to Aβ1–42 fibrils, even when compared to the most viscous condition of 100% glycerol. These signature peaks in both the excitation and emission spectra when bound to Aβ1–42 fibrils can be observed for all of the probes with the exception of p-FTAA-Ph. In addition, similar to the fluorescent amyloid ligand thioflavin T (ThT), all the LCOs displayed an enhanced fluorescence upon binding to amyloid fibrils (Supporting Information Figure S2). Recent studies indicate that the binding of ThT to amyloid fibrils is highly dependent on interactions with the aromatic and hydrophobic sides chains of the protein fibrils.[30,31] Thus, ThT fluorescence is highly sensitive to local interactions occurring when the dye is bound to amyloid fibrils. In addition, it was recently shown that efficient binding of the most conventionally used amyloid ligand, Congo Red, to amyloid fibrils is highly dependent on electrostatic interactions and hydrogen bonding.[32] Most likely such interactions are also relevant for the conformational restriction of the anionic LCOs upon binding to Aβ1–42 fibrils and the interplay of these interactions cannot be completely mimicked by the solvent-only models presented above. However, the solvatochromism and viscosity indices did correlate with the pentameric LCO optical ability to distinguish Aβ and tau deposits. As reported earlier,[12,17] LCOs having carboxyl groups extending the pentameric thiophene backbone, as well as having greater conformational freedom, tend to perform better as probes for the detection of conformational differences between protein aggregates. As shown herein, such LCOs also displayed distinct solvatochromism and decreased Stokes shifts due to increased solvent viscosity. These fundamental photophysical assessments might thus be utilized to predict the LCO ability to act as sensitive optical discriminators of Aβ and tau deposits.

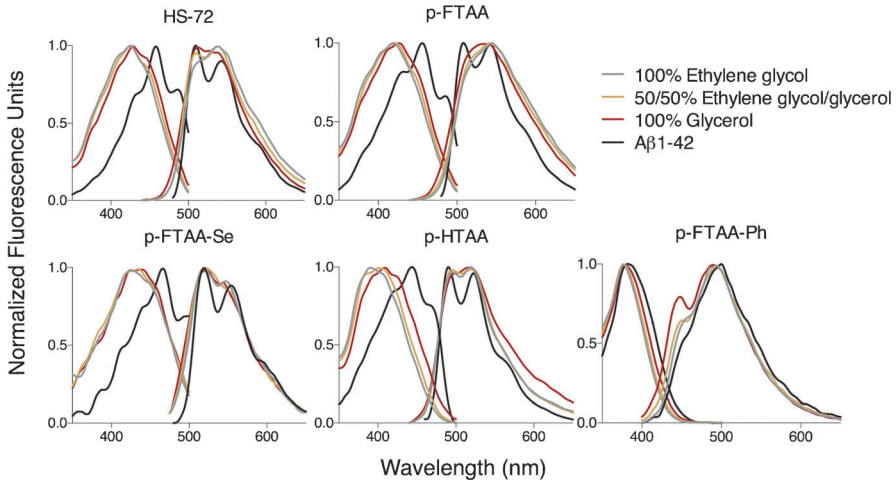

Figure 2. Excitation and emission spectra of 300 nM HS-72, p-FTAA, p-FTAA-Se, p-HTAA and p-FTAA-Ph in 100% ethylene glycol 50% ethylene glycol and 50% glycerol, or 100% glycerol. As a comparison of excitation and emission spectra for the LCOs bound to Aβ1–42 fibrils (10 μM) in PBS are shown (black).

Synthesis and evaluation of three additional LCOs

In order to test our hypothesis that pentameric LCOs for optimal spectral discrimination of Aβ deposits and NFTs should display distinct solvatochromism as well as spectral shifts due to solvent viscosity, three novel anionic pentameric LCO analogues to p-FTAA were synthesized (Figure 3). Firstly, the terminal carboxyl groups were replaced by ketones, resulting in p-KTAA, an anionic pentamer with the same central trimer building block as p-FTAA and neutral polarizable π-acceptor groups (ketones) extending the thiophene backbone instead of negatively charged carboxyl groups. Secondly, the positions of the acetic acid side chains were altered on the trimer building block to render HS-84, an isomer to p-FTAA having the acetic side chains of the trimeric building block tail-to-tail instead of head-to-head. Thirdly, a pentamer (HS-42) lacking the terminal carboxyl groups extending the conjugated backbone, but displaying the same amount of net charge (−4) as p-FTAA was synthesized.

The new LCOs were synthesized in a similar fashion as previously reported.[11,12,17] Thiophene trimer **1**[33] was used as precursor for the synthesis of target compounds p-KTAA and HS-42 (Scheme 1). Electrophilic aromatic substitution on trimer **1** using *N*-bromosuccinimide in DMF gave dibrominated thiophene trimer **2** in 94% yield. Compound **2** was subjected to a Suzuki coupling with 5-acetyl-2-thienylboronic acid (**3**) using K_2CO_3 and the palladium-catalyst PEPPSI™-IPr. Due to solubility problems, after workup, the crude methylester pentamer was subsequently hydrolyzed with 1 M aqueous NaOH in dioxane and water to give p-KTAA in an overall yield of 83% over two steps. Compound **4**[17] was coupled to compound **2** according to the above-mentioned Suzuki conditions affording pentamer **5** in 48% yield. Hydrolysis with 1 M aqueous NaOH in dioxane and water gave HS-42 quantitatively (Scheme 1). The synthetic ap-

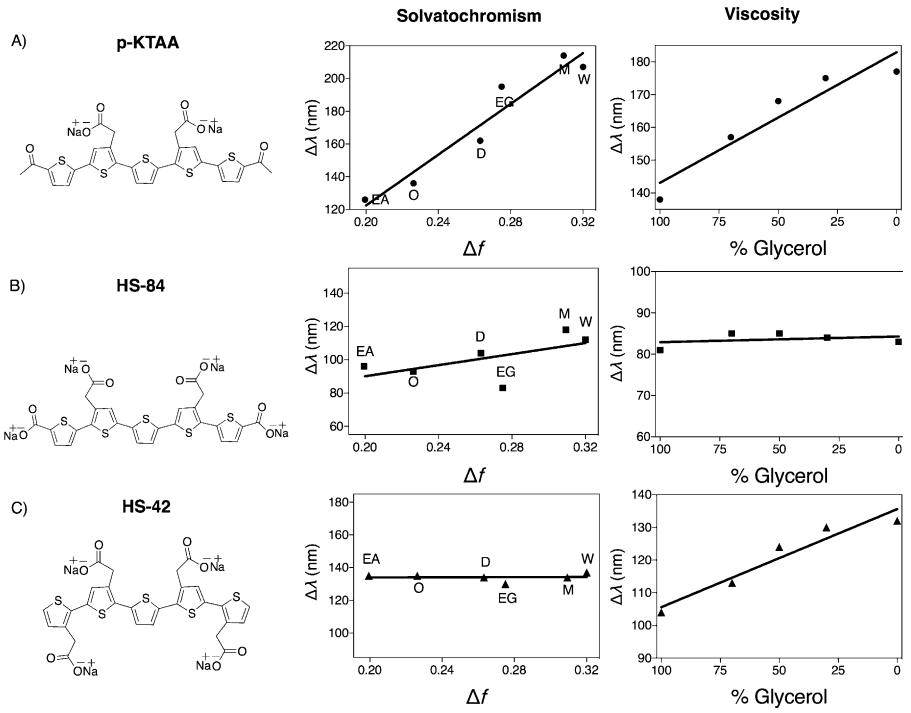

Figure 3. Chemical structures, Lippert–Mataga solvatochromism plots and viscosity plots of the pentameric LCOs: A) p-KTAA, B) HS-84, and C) HS-42. For the solvatochromism, solvents of increasing polarity in the following order: ethyl acetate, octanol, dimethyl sulfoxide (DMSO), ethylene glycol, methanol, and water were used. For the viscosity experiments, LCOs were mixed in solutions of ethylene glycol and glycerol with increasing concentrations of glycerol. The LCO concentration was 300 nM for all experiments.

proach towards pentameric oligothiophene HS-84 required the dimeric thiophene **8** (Scheme 2). This intermediate was prepared according to the same palladium cross-coupling conditions as described above using monomers **6**[33] and **7**, followed by esterification under acidic conditions using methanol as solvent and nucleophile in an overall yield of 71% over two steps. Bromination of the intermediate **8** with *N*-bromosuccinimide in DMF afforded the key precursor **9** in 73% yield. Following the previous procedure dibrominated dimer **9** was coupled to 2,5-thiophenediylbisboronic acid (**10**) yielding methyl ester pentamer **11** in 80%. Final hydrolysis as for HS-42 and p-KTAA gave HS-84 quantitatively (Scheme 2). After synthesis and purification, the solvatochromism and viscosity-dependent spectral changes of the dyes were assessed as described above.

The solvatochromic Lippert–Mataga plot for the three novel anionic pentameric LCOs are shown in Figure 3 and the slope values for the respective LCOs are summarized in Table 2. Similar to p-HTAA, HS-42 also displayed low solvent sensitivity due to the absence of terminal carboxyl groups extending the conjugated thiophene backbone. HS-84 showed a similar solvent sensitivity as p-FTAA, verifying that LCOs having terminal carboxyl groups reveal high solvent sensitivity. In addition, p-KTAA displayed an even higher slope value than p-FTAA, verifying that elongation of the conjugated thiophene backbone with polarizable π-acceptor groups other than carboxyl groups, are possible for achieving LCOs displaying high solvent sensibility. In the viscosity plot, HS-42 and p-KTAA showed high slope values, whereas HS-84 lacked the viscosity-induced changes of the Stokes shift (Figure 3, Table 2). Hence, it appears that HS-84 has less conformational freedom along the backbone than p-FTAA, indicating that changing the position of the acetic acid side chains of the trimeric building block from head-to-head to tail-to-tail might induce alternative intramolecular interactions, such as hydrogen bonding or sulfur–oxygen interac-

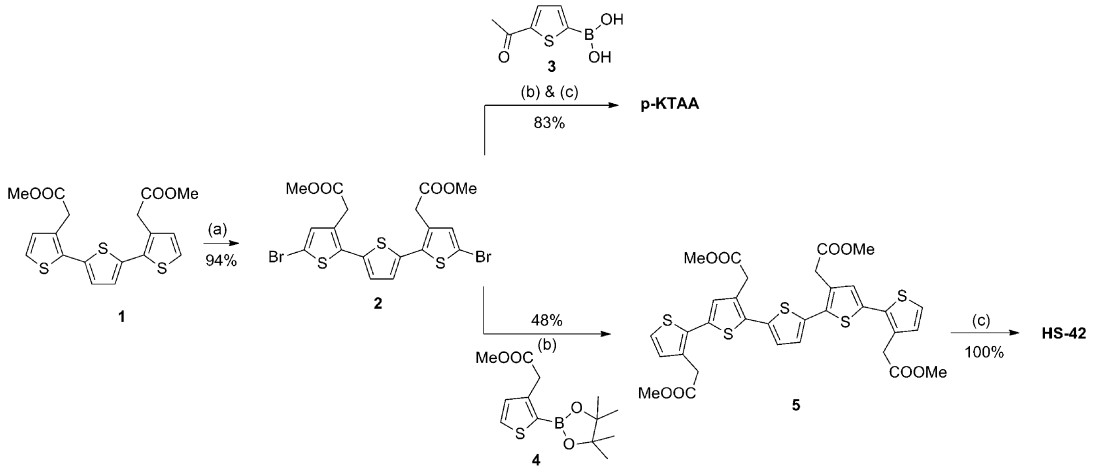

Scheme 1. Synthesis of p-KTAA and HS-42. Reagents and conditions: a) NBS, DMF, 0 °C to RT, 16 h; b) 1,4-dioxane/MeOH, PEPPSI™-IPr, K_2CO_3, 70 °C, 20 min; c) NaOH (1 M), 1,4-doxane, 60 °C, 16 h.

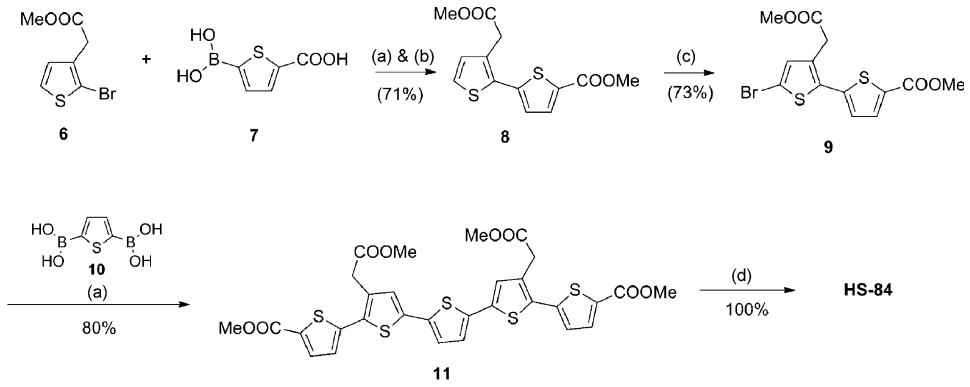

Scheme 2. Synthesis of HS-84. Reagents and conditions: a) 1,4-dioxane/MeOH, PEPPSI™-IPr, K_2CO_3, 70 °C, 20 min; b) MeOH, H_2SO_4, 70 °C, 16 h; c) NBS, DMF, 0 °C to RT, 16 h; d) NaOH (1 M), 1,4-doxane, 60 °C, 16 h.

tions,[34] resulting in backbone rigidity. In addition, it appears that the positioning of acetic acid moieties on adjacent thiophene rings, as in HS-42, induces an increase in steric hindrance between pendant groups without hindering the flexibility of the conjugated backbone. For all the newly synthesized LCOs, the spectral changes that occur upon binding to Aβ1–42 fibrils could not be reproduced by solvent-only restrictions (Supporting Information Figures S3 and S4). Furthermore, all the three LCOs displayed an enhanced fluorescence upon binding to amyloid fibrils (Supporting Information Figure S5). Overall, the results from the solvent experiments predict p-KTAA to be an efficient LCO for spectral discrimination between Aβ and NFTs, while HS-42 and HS-84 should display similar emission profiles for these aggregated species.

To verify the three new pentamers' abilities to distinguish between Aβ and tau deposits, the dyes were utilized for staining of human brain tissue with AD pathology (Figure 4). Indeed, p-KTAA, with the highest solvent sensitivity and the most dynamic range of conformational freedom based on viscosity slopes, proved to be most efficient in terms of ability to spectrally distinguish between immunopositive Aβ deposits and NFTs. p-KTAA bound to Aβ deposits showed an emission maximum around 570 nm, whereas the p-KTAA spectrum from NFTs was red-shifted, having an emission maximum around 595 nm (Figure 4A). Both HS-84 and HS-42 displayed similar emission spectra for the two aggregated entities, verifying that LCOs that are efficient for spectral separation of Aβ deposits and NFTs need to display solvent sensitivity as well as viscosity-induced Stokes shifts. Therefore, the results indicate that the indices of solvent sensitivity (solvatochromism) and conformational freedom (viscosity) can be utilized as predictive determinants for achieving superior LCOs for spectral separation of differing protein aggregates.

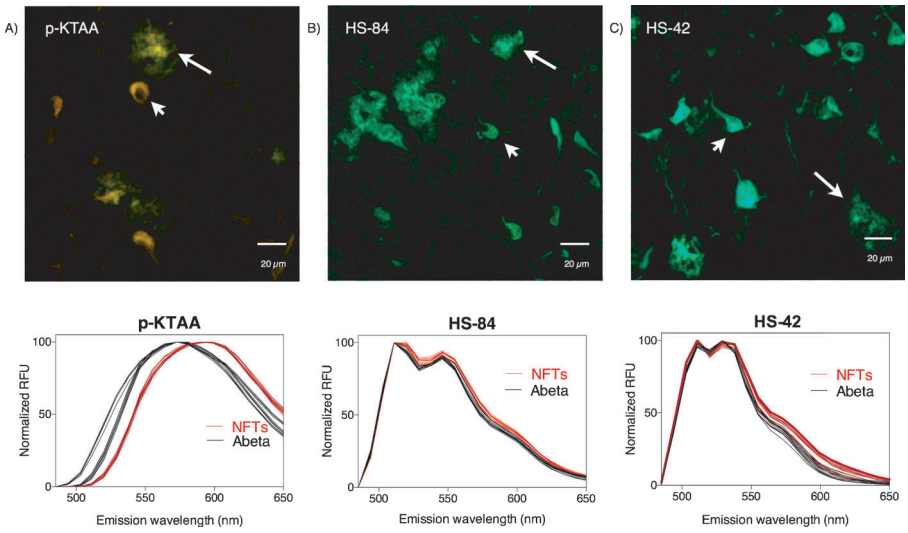

Figure 4. Fluorescence images and emission spectra of: A) p-KTAA, B) HS-84, and C) HS-42 bound to two histopathological hallmarks of AD (Aβ plaques and NFTs) in human brain tissue. The emission spectra of the indicated ligand bound to Aβ plaques or NFTs when excited at 488 nm. The images show the typical pathological protein entities of AD, Aβ plaques (white arrows) and NFTs (white arrow heads), from which the emission spectra were obtained. Scale bars represent 20 μm.

Table 2. Slope values of Lippert–Mataga plots for additional pentamers.

LCO	Slope: solvent	Slope: viscosity
p-KTAA	774.6	39.8
HS-84	166.1	1.4
HS-42	1.85	30.0

Conclusion

Herein, we show that LCOs that are able to spectrally distinguish Aβ deposits and NFTs display distinct solvatochromism as well as viscosity-dependent optical transitions. In addition, the spectral transitions that arise from the LCO interactions with specific protein aggregates are most likely due to differences in binding pocket polarities and the conformational restrictions of the respective protein aggregates. Overall, we have demonstrated that a combination of basic photophysical assessments can facilitate the chemical design of novel thiophene-based ligands that can distinguish different protein ag-

gregate topologies. The results presented also underline that the microenvironment in the binding pockets of distinct protein aggregates differ and this should be considered when designing protein aggregate specific ligands.

Experimental Section

Full experimental details including additional characterization data and NMR spectra of new compounds are given in the Supporting Information. Frozen brain tissues from clinically and neuropathologically well-characterized cases of AD were obtained from the Alzheimer's Disease Research Center, Mount Sinai School of Medicine, New York NY 10029, USA and informed consent for brain donation was obtained from the next-of- kin.

Acknowledgements

Our work is supported by the Swedish Foundation for Strategic Research (K.P.R.N, R.S.) and the Alzheimer Disease Research Center (ADRC) (NIH grantNIH-AG05138; V.H., S.G.). K.P.R.N is financed by an ERC Starting Independent Researcher Grant (Project: MUMID) from the European Research Council. R.S. is enrolled in the doctoral program Forum Scientum.

Keywords: fluorescence · imaging agents · luminescent conjugated oligothiophenes · protein aggregates · solvatochromism

[1] H.-A. Ho, A. Najari, M. Leclerc, *Acc. Chem. Res.* **2013**, *46*, 168 – 178.
[2] S. W. Thomas, G. D. Joly, T. M. Swager, *Chem. Rev.* **2007**, *107*, 1339 – 1386.
[3] C. Zhu, L. Liu, Q. Yang, F. Lv, S. Wang, *Chem. Rev.* **2012**, *112*, 4687 – 4735.
[4] B. Liu, G. C. Bazan, *Chem. Mater.* **2004**, *16*, 4467 – 4476.
[5] K. P. R. Nilsson, J. Rydberg, L. Baltzer, O. Inganäs, *Proc. Natl. Acad. Sci. USA* **2003**, *100*, 10170 – 10174.
[6] K. P. R. Nilsson, P. Hammarström, F. Ahlgren, A. Herland, E. A. Schnell, M. Lindgren, G. T. Westermark, O. Inganäs, *ChemBioChem* **2006**, *7*, 1096 – 1104.
[7] K. P. R. Nilsson, A. Åslund, I. Berg, S. Nyström, P. Konradsson, A. Herland, O. Inganäs, F. Stabo-Eeg, M. Lindgren, G. T. Westermark, L. Lannfelt, L. N. Nilsson, P. Hammarström, *ACS Chem. Biol.* **2007**, *2*, 553 – 560.
[8] C. J. Sigurdson, K. P. R. Nilsson, S. Hornemann, G. Manco, M. Polymenidou, P. Schwarz, M. Leclerc, P. Hammarström, K. Wüthrich, A. Aguzzi, *Nat. Methods* **2007**, *4*, 1023 – 1030.
[9] F. Chiti, C. M. Dobson, *Annu. Rev. Biochem.* **2016**, *75*, 333 – 366.
[10] M. Stefani, C. Dobson, *J. Mol. Med.* **2003**, *81*, 678 – 699.
[11] A. Åslund, C. J. Sigurdson, T. Klingstedt, S. Grathwohl, T. Bolmont, D. L. Dickstein, E. Glimsdal, S. Prokop, M. Lindgren, P. Konradsson, D. M. Holtzman, P. R. Hof, F. L. Heppner, S. Gandy, M. Jucker, A. Aguzzi, P. Hammarström, K. P. R. Nilsson, *ACS Chem. Biol.* **2009**, *4*, 673 – 684.
[12] T. Klingstedt, A. Åslund, R. A. Simon, L. B. G. Johansson, J. J. Mason, S. Nyström, P. Hammarström, K. P. R. Nilsson, *Org. Biomol. Chem.* **2011**, *9*, 8356.
[13] B. M. Wegenast-Braun, A. Skodras, G. Bayraktar, J. Mahler, S. K. Fritschi, T. Klingstedt, J. J. Mason, P. Hammarström, K. P. R. Nilsson, C. Liebig, M. Jucker, *Am. J. Pathol.* **2012**, *181*, 1953 – 1960.
[14] V. Mahajan, T. Klingstedt, R. Simon, K. P. R. Nilsson, A. Thueringer, K. Kashofer, J. Haybaeck, H. Denk, P. M. Abuja, K. Zatloukal, *Gastroenterology* **2011**, *141*, 1080 – 1090.
[15] T. Klingstedt, C. Blechschmidt, A. Nogalska, S. Prokop, B. Häggqvist, O. Danielsson, W. K. Engel, V. Askanas, F. L. Heppner, K. P. R. Nilsson, *ChemBioChem* **2013**, *14*, 607 – 616.
[16] S. Nyström, K. M. Psonka-Antonczyk, P. G. Ellingsen, L. B. G. Johansson, N. Reitan, S. Handrick, S. Prokop, F. L. Heppner, B. M. Wegenast-Braun, M. Jucker, M. Lindgren, B. T. Stokke, P. Hammarström, K. P. R. Nilsson, *ACS Chem. Biol.* **2013**, *8*, 1128 – 1133.
[17] T. Klingstedt, H. Shirani, K. O. A. Åslund, N. J. Cairns, C. J. Sigurdson, M. Goedert, K. P. R. Nilsson, *Chem. Eur. J.* **2013**, *19*, 10179 – 10192.
[18] A. Taghavi, S. Nasir, M. Pickhardt, R. Heyny-von Haussen, G. Mall, E. Mandelkow, E. M. Mandelkow, B. Schmidt, *J. Alzheimer's Dis.* **2011**, *27*, 835 – 843.
[19] M. Maruyama, H. Shimada, T. Suhara, H. Shinotoh, B. Ji, J. Maeda, M. R. Zhang, J. Q. Trojanowski, V. M. Lee, M. Ono, K. Masamoto, H. Takano, N. Sahara, N. Iwata, N. Okamura, S. Furumoto, Y. Kudo, Q. Chang, T. C. Saido, A. Takashima, J. Lewis, M. K. Jang, I. Aoki, H. Ito, M. Higuchi, *Neuron* **2013**, *79*, 1094 – 1108.
[20] K. Cao, M. Farahi, M. Dakanali, W. M. Chang, C. J. Sigurdson, E. A. Theodorakis, J. Yang, *J. Am. Chem. Soc.* **2012**, *134*, 17338 – 17341.
[21] M. Y. Berezin, H. Lee, W. Akers, S. Achilefu, *Biophys. J.* **2007**, *93*, 2892 – 2899.
[22] K. Kudo, A. Momotake, Y. Kanna, Y. Nishimura, T. Arai, *Chem. Commun.* **2011**, *47*, 3867 – 3869.
[23] R. Mishra, D. Sjölander, P. Hammarström, *Mol. Biosyst.* **2011**, *7*, 1232 – 1240.
[24] J. R. Lakowicz, *Principles of Fluorescence Spectroscopy*, Springer, Heidelberg, **2007**.
[25] M. Sheves, K. Nakanishi, B. Honig, *J. Am. Chem. Soc.* **1979**, *101*, 7086 – 7088.
[26] R. Rajamani, Y.-L. Lin, J. Gao, *J. Comput. Chem.* **2011**, *32*, 854 – 865.
[27] A. Fin, A. Vargas Jentzsch, N. Sakai, S. Matile, *Angew. Chem.* **2012**, *124*, 12908 – 12911; *Angew. Chem. Int. Ed.* **2012**, *51*, 12736 – 12739.
[28] D. Alonso Doval, S. Matile, *Org. Biomol. Chem.* **2013**, *11*, 7467 – 7471.
[29] M. A. Haidekker, T. P. Brady, D. Lichlyter, E. A. Theodorakis, *Bioorg. Chem.* **2005**, *33*, 415 – 425.
[30] M. Biancalana, K. Makabe, A. Koide, S. Koide, *J. Mol. Biol.* **2009**, *385*, 1052 – 1063.
[31] M. Biancalana, S. Koide, *Biochim. Biophys. Acta* **2010**, *1804*, 1405 – 1412.
[32] A. K. Schütz, A. Soragni, S. Hornemann, A. Aguzzi, M. Ernst, A. Böckmann, B. H. Meier, *Angew. Chem.* **2011**, *123*, 6078 – 6082; *Angew. Chem. Int. Ed.* **2011**, *50*, 5956 – 5960.
[33] A. Åslund, A. Herland, P. Hammarström, K. P. R. Nilsson, B.-H. Jonsson, O. Inganäs, P. Konradsson, *Bioconjugate Chem.* **2007**, *18*, 1860 – 1868.
[34] H. J. Spencer, P. J. Skabara, M. Giles, I. McCulloch, S. J. Coles, M. B. Hursthouse, *J. Mater. Chem.* **2005**, *15*, 4783 – 4792.

Received: April 1, 2014
Published online on August 8, 2014

